Synthesis and Structure of $K_{10}Tl_7$: The First Binary Trielide Containing Naked Pentagonal Bipyramidal Tl_7 Clusters

Stefan Kaskel and John D. Corbett*

Ames Laboratory—DOE and Department of Chemistry, Iowa State University, Ames, Iowa 50011

Received October 4, 1999

The title compound is synthesized by direct fusion of the elements at 400 °C followed by annealing at 330 °C, quenching to room temperature, and subsequent annealing at 120 and 100 °C for days to weeks. The compound crystallizes in the monoclinic space group $P2_1/c$ (No. 14), with $Z = 4$, $a = 10.132(1)$ Å, $b = 22.323(2)$ Å, $c = 13.376(1)$ Å, and $\beta = 93.14(1)°$, and consists of Tl_7^{7-} clusters embedded in a matrix of potassium ions. The cluster is an axially compressed pentagonal bipyramid close to D_{5h} symmetry. The apex−apex bond distance (3.462(1) Å) is little longer than the bonds in the pentagonal waist (3.183(1)−3.247(1) Å). Structurally the compound is not electron-precise: $K_{10}Tl_7$ has three extra electrons per Tl_7 cluster and is Pauli paramagnetic ($\chi_{300} = 2.25 \times 10^{-4}$ emu/mol).

Introduction

In recent years, the heavy elements of group 13 have been shown to be prolific in the formation of new polyanionic cluster compounds with alkali, alkaline-earth, or even rare-earth metals acting as electron-donating counterions.[2] Whereas gallium more often tends to form anionic cluster networks, thallium shows a great variety of isolated cluster anions. The homoatomic thallium clusters can be divided into three groups: *nido*-Tl_4^{8-} in Na_2Tl,[3] *closo*-Tl_5^{7-} in $Na_2K_{21}Tl_{19}$,[4] and *closo*-Tl_6^{8-} in $Na_{14}K_6Tl_{18}M$ (M = Mg, Zn, etc.)[5] can be regarded as new examples of Wade's-rule (electron-deficient) clusters in which a formal lone pair is present at each vertex instead of the *exo* B−H bond in the boranes.[2] The Tl_{13}^{11-} in $Na_3K_8Tl_{13}$[6] is also a closo but a Tl-centered icosahedron. The apparent formal charges on the clusters should only be regarded as oxidation state accountings, recognizing that covalent as well as Coulombic interactions between the ions play important roles in stabilizing these compounds.

Another class is found in clusters such as Tl_6^{6-} in KTl[7] and Tl_{11}^{7-} in K_8Tl_{11}.[8] These anions resemble *closo*-polyhedra but are considerably distorted in comparison, presumably in order to reduce relatively high negative charges. These clusters are thus more electron-deficient compared with the Wade formalism and are often referred to as *hypoelectronic*. Tl_9^{9-} in $Na_2K_{21}Tl_{19}$[4] is an example of a third class of trielide anions that can be viewed as an icosahedral, centered Tl_{13} cluster from which four adjoining vertexes have been removed.

Following the recent discovery of another example of a hypoelectronic cluster, the Tl_7^{7-} in the complex $(Na^+)_{12}(K^+)_{38}(Tl_7^{7-})_3(Tl_9^{9-})_3(Au^-)_2$,[9] we now report a second simpler compound containing these compressed pentagonal bipyramidal Tl_7 clusters, in this case in the new binary phase $K_{10}Tl_7$. This compound is the potassium-richest phase in the K−Tl phase diagram and was initially detected as a side product in the synthesis of KTl.[7] According to extended Hückel calculations, $K_{10}Tl_7$ must have three extra delocalized electrons per formula unit and metallic properties.

Experimental Section

The general techniques utilizing welded Ta tubing containers, glovebox operations, and Guinier powder diffraction techniques have been described before.[7] An improved method of sample preparation for powder pattern measurement mounts the powder between two thin sheets of aluminum-coated polyester foil. A thin film of grease is used to hold the sample and to seal the outer edge of the foil to prevent decomposition of the air-sensitive products, much better than with the former cellophane tape. All operations were carried out in N_2- or He-filled gloveboxes.

Syntheses. According to the powder pattern, the title phase is obtained in ~90% yield (together with ~10% KTl) following direct fusion of stoichiometric amounts of the elements (K, 99.95% Alfa-Aesar; Tl, 99.998% Johnson Matthey) at 400 °C for 48 h followed first by annealing at 330 °C for 12 h. The container is then quenched to room temperature by water and later annealed at 120 °C (14 days) and 100 °C (7 days). This procedure gives a brittle gray metallic-appearing product. In air, the compound immediately decomposes and turns black, and only white and gray products remain after 30 min. Only thallium metal was identified for certain as a decomposition product according to the powder pattern. The white residue is probably KOH.

Single crystals appropriate for structural analyses were obtained from a potassium-richer sample ($K_{37}Tl_7$). This was homogenized at 400 °C for 48 h, quenched to room temperature, and annealed at 150 °C for 8 weeks. After slow cooling to 60 °C (at 5 °C/day), the furnace was turned off. The sample contained brownish single crystals in a rather soft matrix of potassium metal. The eutectic point is about 60 °C and 1 atom % Tl.[10] Crystals were cut out of the sticky material with a

(1) This research was supported in part by the Office of Basic Energy Sciences, Materials Sciences Division, U.S. Department of Energy. Ames Laboratory is operated for DOE by Iowa State University under Contract No. W-7405-Eng-82.
(2) Corbett, J. D. In *Chemistry, Structure and Bonding of Zintl Phases and Ions*; Kauzlarich, S. M., Ed.; VCH Publishers: New York, 1996; Chapter 4.
(3) Smith, F.; Hansen, D. A. *Acta Crystallogr.* **1967**, *22*, 836.
(4) Dong, Z.-C.; Corbett, J. D. *J. Am. Chem. Soc.* **1994**, *116*, 3429.
(5) Dong, Z.-C.; Corbett, J. D. *Angew. Chem., Int. Ed. Engl.* **1996**, *35*, 1006.
(6) Dong, Z.-C.; Corbett, J. D. *J. Am. Chem. Soc.* **1995**, *117*, 6447.
(7) Dong, Z.-C.; Corbett, J. D. *J. Am. Chem. Soc.* **1993**, *115*, 11299.
(8) Cordier, G.; Müller, V. *Z. Kristallogr.* **1992**, *198*, 281.
(9) Huang, D.-P.; Dong, Z.-C.; Corbett, J. D. *Inorg. Chem.* **1998**, *37*, 5881.

10.1021/ic991168s CCC: $19.00
Published on Web 01/26/2000

scalpel, cleaned of K metal, and mounted in capillaries. Bulk samples obtained by this method also contained KTl according to the powder pattern. KTl crystals were even found in K-richer samples ($K_{55}Tl_7$) so treated, as identified by their lattice constants (20 reflections indexed on a single-crystal diffractometer). Powder patterns of different parts of samples gave evidence for inhomogeneities depending on the temperature treatment.

A sample loaded as $K_{55}Tl_7$ (60 wt % K) was slowly cooled from 400 °C (0.05 °C/min) to room temperature. According to the phase diagram,[10] this should preclude formation of KTl if the peritectic decomposition temperature of $K_{10}Tl_7$ is above 230 °C, but instead only about 40% $K_{10}Tl_7$ was formed according to the powder pattern. Obviously, the crystallization temperature of $K_{10}Tl_7$ is lower, and since annealing procedures below 150 °C resulted in highest yields, this temperature is probably a good approximation for the peritectic formation of $K_{10}Tl_7$. These considerations are in agreement with the observed inhomogeneities: during slower cooling from 400 °C, the Tl-richer KTl precipitates first, and these crystals have enough time to segregate to the bottom of the tube (assuming their density is higher than that of the melt). An analogue of this process on a larger scale can be found in Bowen's discontinuous differentiation of magmatic rocks.[11]

Experiments under dynamic vacuum were carried out in order to ascertain that no hydride impurities were present. To remove hydrogen, three samples sealed in Ta were heated in a dynamic vacuum to 600, 700, or 900 °C for 24 h, held at 400 °C for at least 24 h, and then either slowly cooled or quenched and annealed at lower temperatures (130−150 °C) for some days. All samples produced at least 40% $K_{10}Tl_7$. Addition of 1 mol or even 3 mol of KH per mole of $K_{10}Tl_7$ also did not significantly improve the yield of $K_{10}Tl_7$. These samples were heated to 400 °C for 2 days and then quenched and annealed at 150 °C for 10 days. Moreover, addition of excess KH after quenching a $K_{10}Tl_7$ mixture to room temperature and subsequent annealing gave no significantly improved yield. The compound is therefore considered to be hydrogen free and a true binary.

The KH was prepared[12] by the reaction of K metal with static hydrogen that had been purified by passage through a dry ice-cooled trap. The metal was placed in a 12 mm i.d. Ta container that was sealed at one end, inserted in a Pyrex tube, and slowly heated to 400 °C (0.8 °C/min), under hydrogen. After cooling, KH was obtained as a fluffy white material, the purity of which was proven by X-ray powder diffraction.

X-ray Diffraction. Crystals of $K_{10}Tl_7$ were sealed in capillaries in a N_2-filled glovebox and checked for singularity by Laue photographs. X-ray intensity data were measured at 23 °C on a Bruker SMART1000 CCD-based X-ray diffractometer system equipped with a Mo X-ray tube; 1027 frames were collected with an exposure time of 60 s/frame. These were integrated with the Siemens SAINT software package for the monoclinic unit cell initially obtained by indexing 149 reflections. This process yielded a total of 15017 reflections out of which 6960 were independent and 2986 had intensities greater than $2\sigma(I)$.

The XPREP subprogram was used for the space group determination, in which systematic absences indicated the space group $P2_1/c$. The Tl positions were obtained by direct methods whereas the K positions were found in the difference Fourier map. Data were corrected for absorption ($\mu = 385.6$ cm^{-1}) using the SADABS program[13] to give minimum and maximum relative transmission coefficients of 0.464 and 1.0, respectively. The refinement converged after anisotropical refinement of all atoms with R1 = 0.046 and wR2 (on F_o^2) = 0.065. The largest residuals in the final difference Fourier map were 1.76 and −2.12 e$^-$/Å^3. The cell constants $a = 10.132(1)$ Å, $b = 22.323(2)$ Å, $c = 13.376(2)$ Å, and $\beta = 93.14(1)°$ are based upon least squares refinement of 43 lines measured in the Guinier powder pattern with the aid of NIST silicon as an internal standard. Some general parameters are listed in Table 1, while more details and the anisotropic thermal parameters are in the Supporting Information.

Table 1. Some Collection and Refinement Parameters for $K_{10}Tl_7$

fw	1821.59
cryst syst, space group, Z	monoclinic, $P2_1/c$ (No. 14), 4
unit cell dimens (Å, deg)[a]	$a = 10.132(1)$
	$b = 22.323(2)$
	$c = 13.376(2)$
	$\beta = 93.14(1)$
V (Å^3)	3021(1)
ρ_{calcd}, g cm^{-3}	4.005
μ (Mo Kα, cm^{-1})	385.60
R1, wR2[b]	0.046, 0.065

[a] Guinier powder pattern, 43 lines, $\lambda = 1.540\,562$, 23 °C. [b] $R1 = \sum||F_o| - |F_c||/\sum|F_o|$, $wR2 = \{\sum[w(F_o^2 - F_c^2)^2]/\sum[w(F_o^2)^2]\}^{1/2}$.

Magnetic Measurements. Magnetic susceptibilities were measured on a Quantum Design SQUID magnetometer between 6 and 296 K at a field of 3 T. A 43.1 mg sample with a $K_{10}Tl_7$:KTl weight ratio of 9:1 according to the powder pattern was loaded into a silica tube in a helium-filled glovebox. The sample was held between two silica rods within the silica tube, and the apparatus was sealed under a low static pressure. The initial composition of the sample was $K_{10}Tl_7$, so a small amount of K metal, usually not detectable by means of powder diffraction, could be estimated from the loaded composition and the observed $K_{10}Tl_7$:KTl ratio. Thus, after subtraction of the diamagnetic contribution of the sample holder, the magnetization was corrected for 9.9 wt % of diamagnetic KTl ($\chi_{mol,uncorr} = -8 \times 10^{-5}$ emu/mol[7]) and 0.7 wt % of paramagnetic K ($\chi_{mol} = 2.08 \times 10^{-5}$ emu/mol[14]). The susceptibility data were finally corrected for the diamagnetic contributions of the K and Tl cores in $K_{10}Tl_7$ (-3.68×10^{-4} emu/mol). The corrected susceptibility of $K_{10}Tl_7$ at 300 K is 2.25×10^{-4} emu/mol, with a variation over the 6−300 K range of 16%. If impurities were not taken into account, this value would be reduced by 19%.

EHMO Calculations. MO calculations for the isolated Tl_7 cluster were performed at the extended Hückel level with the program package CAESAR developed by Whangbo and co-workers.[15] For symmetry considerations and simplification, an idealized pentagonal bipyramid was constructed with an apex−apex distance of $d_{aa} = 3.46$ Å, equal distances between neighboring Tl atoms in the pentagonal waist, 3.20 Å, and apex−waist distances of 3.22 Å. The coulomb integrals used came from density functional theory (6s, −11.525; 6p, −5.715 eV[16]), and the orbital coefficients were obtained from SCF calculations (6s, 2.14; 6p, 2.04[17]).

Results and Discussion

Structure. The atomic positions for $K_{10}Tl_7$ are given in Table 2, and the more important distances are in Table 3. The structure of $K_{10}Tl_7$, Figure 1, consists of anionic Tl_7 clusters that are embedded in a loose matrix of potassium cations. The anion is an oblate pentagonal bipyramid, close in geometry to the Tl_7 cluster recently found in the more complex $Na_{12}K_{38}Tl_{48}Au_2$.[9] Although the latter is considerably distorted from D_{5h} symmetry, with bond distances in the pentagonal plane varying between 3.206 and 3.389 Å, our new example in $K_{10}Tl_7$, Figure 2, is less distorted with extreme distances in the plane of 3.183 and 3.247 Å. The average bond length in the equatorial pentagon is $\bar{d}_{ee} = 3.207$ Å. The 5-fold axis is almost parallel to the c axis, and the apex−apex bond is only little longer than before, 3.462(1) Å (Tl1−Tl2, d_{aa}), whereas the average apex−waist distance $\bar{d}_{ea}$ is 3.231 Å. The ratio $d_{aa}/\bar{d}_{ee} = 1.080$ can be used as a measure of the cluster's compression or elongation. The earlier

(10) Thümmel, R.; Klemm, W. *Z. Anorg. Allg. Chem.* **1970**, *376*, 44.
(11) Press: F.; Siever, R. *Understanding earth*; W. H. Freeman and Co.: New York, 1994; p 80.
(12) Brauer, G. *Handbook of Preparative Inorganic Chemistry*, 2nd ed.; Academic Press: New York, 1965; p 971.
(13) Blessing, R. H. *Acta Crystallogr.* **1995**, *A51*, 33.
(14) Klemm, W.; Hauschulz, B. *Z. Elektrochem.* **1939**, *45*, 346.
(15) Ren, J.; Liang, W.; Whangbo, M.-H. *CAESAR for Windows*; Prime-Color Software, Inc., North Carolina State University: Raleigh, NC, 1998.
(16) Vela, A.; Gázquez, J.-L. *J. Phys. Chem.* **1988**, *92*, 5688.
(17) Clementi, E.; Raimondi, D. L.; Reinhardt, W. P. *J. Chem. Phys.* **1967**, *47*, 1300.

Table 2. Atomic Coordinates ($\times 10^4$) and Equivalent Isotropic Displacement Parameters (Å^2 $\times$ 10^3) for $K_{10}Tl_7$

atom	*x*	*y*	*z*	B_{eq}[a]
Tl1	484(1)	3720(1)	3748(1)	29(1)
Tl2	−431(1)	3784(1)	1218(1)	35(1)
Tl3	2193(1)	4470(1)	2246(1)	38(1)
Tl4	−812(1)	2604(1)	2530(1)	36(1)
Tl5	−711(1)	4910(1)	2746(1)	37(1)
Tl6	2149(1)	3047(1)	2078(1)	39(1)
Tl7	−2572(1)	3763(1)	2919(1)	42(1)
Kl	4289(4)	3712(3)	4137(3)	52(2)
K2	1785(6)	2165(2)	4425(3)	55(2)
K3	1867(5)	5299(2)	4711(3)	52(1)
K4	1412(5)	3551(2)	6455(3)	48(2)
K5	5476(5)	5221(3)	2664(4)	59(2)
K6	−1967(6)	2698(3)	5040(3)	56(2)
K7	−1618(6)	3937(2)	−1664(4)	59(2)
K8	−4615(6)	2281(3)	2435(4)	61(2)
K9	5135(5)	3775(3)	812(4)	71(2)
K10	1876(6)	4751(3)	−325(4)	67(2)

[a] B_{eq} is defined as one-third of the trace of the orthogonalized $\mathbf{U}_{ij}$ tensor.

Table 3. Selected Bond Distances in $K_{10}Tl_7$ (Å)

Within the Tl_7 Cluster					
Apex−Apex					
Tl1−Tl2	3.4622(9)				
Apex−Base					
Tl1−Tl3	3.197(1)	Tl1−Tl7	3.232(1)	Tl2−Tl6	3.246(1)
Tl1−Tl4	3.217(1)	Tl2−Tl4	3.202(1)	Tl2−Tl5	3.261(1)
Tl1−Tl5	3.185(1)	Tl2−Tl7	3.229(2)	Tl2−Tl3	3.301(1)
Tl1−Tl6	3.240(1)				
Pentagonal Base					
Tl5−Tl7	3.196(1)	Tl3−Tl5	3.208(1)	Tl4−Tl6	3.247(1)
Tl3−Tl6	3.183(1)	Tl4−Tl7	3.202(1)		
K−Tl within $K_{22}Tl_7$ Complex					
Exo K−Tl					
Tl1−K4	3.711(4)	Tl4−K7	3.708(5)	Tl6−K8	3.706(6)
Tl2−K7	3.989(5)	Tl5−K4	3.678(4)	Tl7−K1	3.654(5)
Tl3−K5	3.739(6)				
μ_2-Bridging on Waist Edges					
K4−Tl4	3.761(5)	K7−Tl3	3.681(5)	K8−Tl7	3.938(6)
K4−Tl6	3.730(4)	K7−Tl5	3.830(5)	K9−Tl6	3.903(6)
K5−Tl5	3.921(6)	K8−Tl4	3.916(6)	K9−Tl3	3.948(6)
K5−Tl7	3.815(6)				
μ_2-Bridges on the Lower Half					
K10−Tl2	3.860(6)	K6−Tl2	3.948(5)	K9−Tl7	3.554(5)
K10−Tl3	3.493(5)	K6−Tl4	3.533(5)	K10−Tl2	3.752(6)
K2−Tl2	3.984(5)	K9−Tl2	*4.496(5)*	K10−Tl5	3.468(5)
K2−Tl6	3.580(5)				
μ_3-Bridges on the Upper Half					
K3−Tl1	3.907(5)	K6−Tl4	3.622(5)	K1−Tl6	3.720(5)
K3−Tl7	3.834(5)	K2−Tl1	3.804(5)	K1−Tl3	3.631(5)
K3−Tl5	3.688(5)	K2−Tl4	3.684(5)	K3−Tl1	3.982(5)
K6−Tll	3.850(6)	K2−Tl6	3.740(5)	K3−Tl3	3.812(5)
K6−Tl7	3.726(5)	K1−Tl1	3.862(5)	K3−Tl5	3.706(5)
Shorter K−K (<4.15 Å)					
K1−K5	4.115(8)	K2−K4	4.148(7)	K7−K10	3.976(7)
K1−K8	4.112(8)	K3−K3	4.13(1)	K8−K9	3.982(9)
K2−K6	4.109(9)	K5−K9	4.071(9)	K10−K10	4.10(1)

Tl_7 example with C_{2v} symmetry[9] has a slightly short $\bar{d}_{aa}$, 3.394 Å, a longer $\bar{d}_{ee}$ = 3.290 Å and $d_{aa}/\bar{d}_{ee}$ = 1.032. Presumably the differences and distortions in general arise from packing forces.

The Tl_7 clusters are quite compressed compared with those in the *closo* 2,4-$C_2B_5H_7$,[18] the structure of which was characterized by electron diffraction in the gas phase. This was reported to have d_{aa} = 2.31(1) Å, that is, without a transannular bond, an equatorial d_{BB} of 1.66(1) Å and thus d_{aa}/d_{BB} = 1.40. Further examples of pentagonal bipyramidal clusters with characterized structures are rare, but one gold cluster $[(AuPPh_3)_7]^{+}$ [19] is strongly compressed, $d_{aa}/\bar{d}_{ee}$ = 0.876.

The cations around the new Tl_7 cluster show an astonishingly regular distribution. Each Tl_7 is surrounded by 22 potassium cations, as shown in Figure 3. All K−Tl distances but one fall in a range between 3.493 and 3.989 Å, with K9−Tl2 anomalously long, 4.496(5) Å. Potassium ions are exo bonded at all seven vertexes, and five more bridge edges about the pentagonal waist. On one side of the oblate cluster, five more cations lie

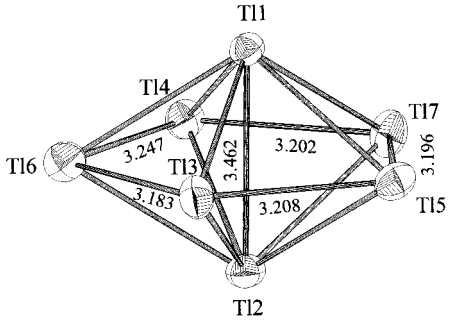

Figure 1. Unit cell of $K_{10}Tl_7$ with Tl_7 clusters embedded in a potassium matrix.

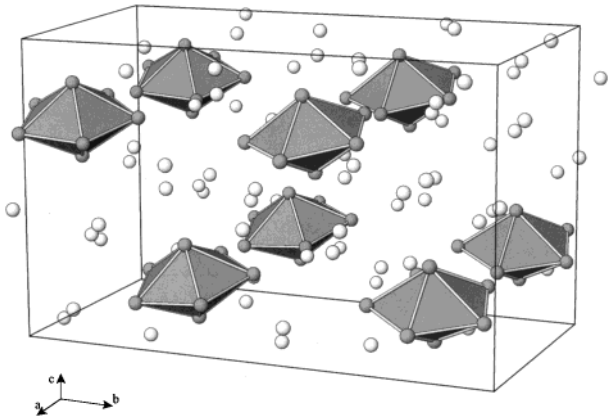

Figure 2. Pentagonal bipyramidal Tl_7 cluster in $K_{10}Tl_7$ (50% ellipsoids).

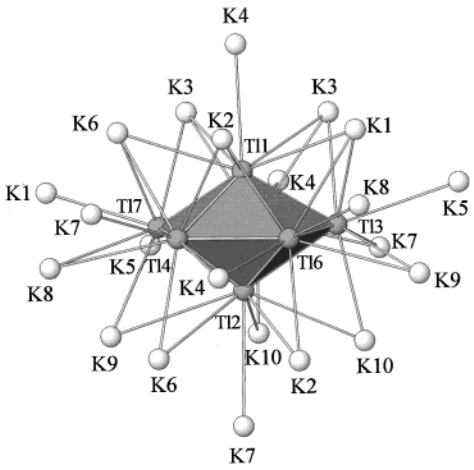

Figure 3. Coordination sphere of K around the Tl_7 cluster, with μ_1, μ_2, and μ_3 functionalities.

(18) McNeill, E. A.; Scholer, F. R. *J. Mol. Struct.* **1975**, *27*, 151.

(19) van der Velden, J. W. A.; Beurskens, P. T.; Bour, J. J.; Bosman, W. P.; Noordik, J. H.; Kolenbrander, M.; Buskes, J. A. K. M. *Inorg. Chem.* **1984**, *23*, 146.

above edges and bridge between axial and equatorial Tl atoms (bottom, Figure 3). These μ_2-bridges are quite asymmetric, with bonds to equatorial Tl 0.3−0.4 Å shorter (Tl3−K10, 3.493(5) Å; Tl4−K6, 3.533(5) Å; Tl5−K10, 3.468(5) Å; Tl6−K2, 3.580-(5) Å; Tl7−K9, 3.554(5) Å). The five remaining cations on the other side of the pentagonal bipyramid make μ_3 caps on the faces. The whole coordination sphere has approximate C_{5v} symmetry. The generally specific cation solvation that is observed about a wide variety of p-metal cluster anions has been described recently.[20] The above order of description (μ_1, μ_2, μ_3) presumably reflects the increase in strength of the cation−anion interactions.

The K cations have coordination numbers of 12−15, 3 to 6 of which are Tl neighbors where they serve to connect the clusters into a three-dimensional network. The exo-bonding K4 and K7 at apexes connect *three* neighboring Tl_7 units whereas all other cations form bridges between *two* clusters. The structure can therefore be described as a three-dimensional condensed network of Tl_7K_{22} clusters, in the Niggli notation as $[^3_\infty Tl_7K_{16/2}K_{6/3}]$.

The packing of the clusters is best described in terms of hcp layers of Tl_7 clusters that lie nearly normal to the *a* axis (Figure 2). The shortest Tl−Tl distance between cluster units in different layers is 5.560 Å. However, packing within the layers is more dense and gives rise to numerous though still fairly distant "contacts", the shortest being 5.594 Å (Tl1−Tl5). This reflects the more numerous links *within* the layers provided through six K ions that connect two or three adjacent clusters compared with only four (K1, K5, K8, K9) that are located *between* two hexagonal layers. In summary, the Tl_7 clusters are well separated from each other in the potassium matrix, and no direct Tl−Tl bonds between clusters are conceivable. Two-thirds of the three shortest K−K separations at 3.98 Å occur within the cluster layers just described and do not appear unusual. These compare with the shortest in K_6Tl_6, 4.05 Å,[7] and three near 4.06 Å in K_8Tl_{11}.[21] One electron per cluster appears to be delocalized in the latter, but evidence for its effects are difficult to discern; the conditions are far removed from those in potassium metal, and those distances are not useful for comparison.

Cluster Bonding. The compound $K_{10}Tl_7$ affords a further example of a naked anionic cluster that is axially compressed compared with an ideal *closo*-Tl_7 cluster. Consequently, the energies and bonding character of all orbitals with strong radial and tangential contributions along the pseudo-5-fold axis are altered. In the undistorted *closo*-2,4-$C_2B_5H_7$, $2n + 2 = 16$ electrons occupy bonding cluster orbitals, and 14 electrons are needed for the 2e−2c B(C)−H bonds. A similar but uncompressed naked Tl_7 cluster would have 15 bonding molecular orbitals of which seven can be regarded as outward pointing lone pairs or just s-orbitals, and eight are skeletal bonding orbitals, thus generating Tl_7^{9-}.

As a consequence of the compression along the 5-fold axis, the number of bonding orbitals is reduced by one to the result shown in the MO diagram in Figure 4 for the isolated cluster. The $2a_2''$ MO, which is antibonding with respect to the apex−apex bond, Figure 5, is raised in energy on axial compression. With 14 occupied molecular orbitals the formal charge on the cluster anion is 7−. For a Tl_7^{9-} anion, a relative elongation of the cluster along the 5-fold axis would be necessary because of the increasing antibonding character of the $2a_2''$ orbital with respect to a decrease in the apex−apex separation. Identical

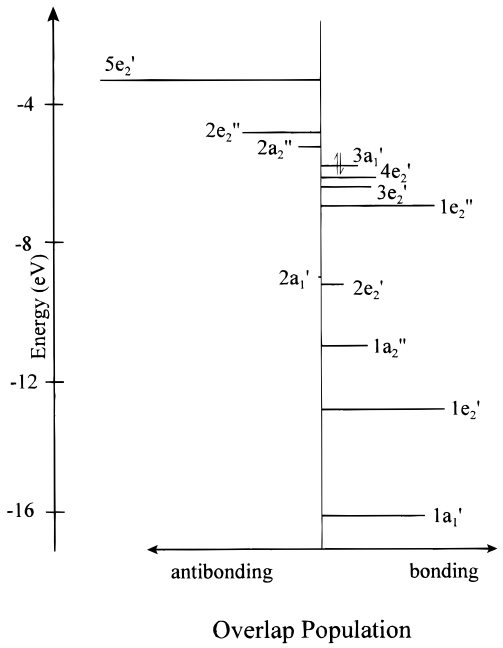

Figure 4. MO scheme for the Tl_7^{7-} anion showing both the energies and the relative overlap populations of each. The HOMO is the marked $3a_1'$. The calculation is based on the idealized D_{5h} symmetry.

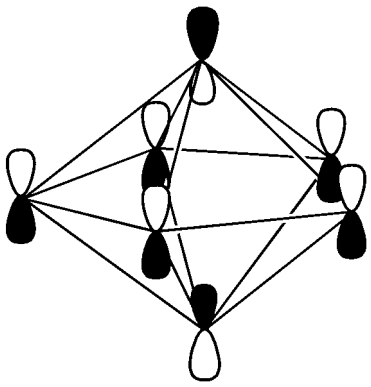

Figure 5. Linear combination of atomic orbitals for the $2a_2''$ LUMO of the Tl_7^{7-} cluster, based on the ideal D_{5h} ion.

bonding considerations were already developed for the formal charge balancing in $(Na^+)_{12}(K^+)_{38}(Tl_7^{7-})_3(Tl_9^{9-})_3(Au^-)_2$.[9] Analogously compressed polyhedra were discovered in the thallides $(A^+)_6(Tl_6^{6-})$, A = K, Cs,[7,22] in which the number of bonding orbitals is also reduced by one compared with that in the regular *closo*-Tl_6^{8-}.

Surprisingly, the proposed bonding scheme for just the ions in $K_{10}Tl_7$ does not result in electronic balance, viz., as K_7Tl_7, a composition that in fact yields the above K_6Tl_6 instead. Rather three extra electrons remain. Also, synthesis efforts as well as the small residual electron densities found in the structural solution indicate the absence of significant amounts of hydrogen, oxygen, nitrogen, or other contaminants. The three electrons instead must occupy a conduction band which is mainly potassium 4s in character. This is not immediately evident from the simple MO scheme, Figure 4, since the antibonding $2a_2''$ and $2e_2''$ MO would have lower energies (−5.26 and −4.75 eV, respectively) than the 4s level on an isolated potassium atom (−4.52 eV[15]). However, we have used the valence state ionization energies of only the neutral thallium atoms in our calculations because inclusion of, and charge iteration for, alkali-

(20) Corbett, J. D. *Angew. Chem., Int. Ed.*, in press.
(21) Dong, Z.-C.; Corbett, J. D. *J. Cluster Sci.* **1995**, *6*, 187.
(22) Dong, Z.-C.; Corbett, J. C. *Inorg. Chem.* **1996**, *35*, 2301.

metal cations is of questionable significance. The anionic character of the cluster is therefore not explicitly included in our MO picture nor is the important Madelung energy of the system, which would certainly alter the energetic relationships to one appropriate to the ions, plus of course some small degree of covalence.[23] In the former part, the −1 oxidation state for thallium would cause its valence and cluster MO levels to be elevated so as to lie above a lower energy appropriate to an oxidized potassium. The predicted metallic character of $K_{10}Tl_7$ is in agreement with the observed net Pauli-like paramagnetism, $\chi_{mol} = 2.2(1) \times 10^{-4}$ emu/mol at 300 K.

$K_{10}Tl_7$ is a further example of a *sub-thallide* in which the number of cations and electrons do not meet expectations for a closed-shell anion, doubtlessly because of improved packing and binding achieved with the three extra potassium atoms. The first member of this class of new and unexplored compounds was A_8Tl_{11} (A = K, Rb, Cs)[8,21] which consists of hypoelectronic Tl_{11}^{7-} anions, one extra cation, and evidently one delocalized electron per formula unit. The term "metallic Zintl phase" has been suggested as a useful descriptor for such compounds in which the cluster anion fulfills the simple electronic requirements for its bonding in the presence of excess free electrons.[2,20,24] This characteristic is being recognized with increased frequency in intermetallic and similar systems.

Acknowledgment. We thank the Alexander von Humboldt Foundation who enabled S.K. to work on this project within the scope of a Feodor Lynen Research Fellowship. J. Ostenson measured the magnetic susceptibility data.

Supporting Information Available: Tables with more data collection and refinement information and the anisotropic thermal parameters for $K_{10}Tl_7$. This material is available free of charge via the Internet at http://pubs.acs.org.

IC991168S

(23) Miller, G. J. In *Chemistry, Structure and Bonding of Zintl Phases and Ions*; Kauzlarich, S. M., Ed.; VCH Publishers: New York, 1996; p 13.

(24) Nesper, R. *Prog. Solid State Chem.* **1990**, *20*, 1.